





## ARTICLE

# Applied physiologically-based pharmacokinetic modeling to assess uridine diphosphate-glucuronosyltransferase-mediated drug–drug interactions for Vericiguat

Sebastian Frechen<sup>1</sup>  | Ibrahim Ince<sup>1</sup> | André Dallmann<sup>1</sup>  | Michael Gerisch<sup>2</sup>  |  
 Natalia A. Jungmann<sup>2</sup> | Corina Becker<sup>3</sup> | Maximilian Lobmeyer<sup>3</sup> |  
 Maria E. Trujillo<sup>4</sup> | Shiyao Xu<sup>4</sup> | Rolf Burghaus<sup>1</sup>  | Michaela Meyer<sup>1</sup>

<sup>1</sup>Pharmacometrics/Modeling and Simulation, Research and Development, Pharmaceuticals, Bayer AG, Leverkusen, Germany

<sup>2</sup>DMPK, Research and Development, Pharmaceuticals, Bayer AG, Leverkusen, Germany

<sup>3</sup>Clinical Pharmacology, Research and Development, Pharmaceuticals, Bayer AG, Leverkusen, Germany

<sup>4</sup>Merck & Co., Inc., Rahway, New Jersey, USA

## Correspondence

Sebastian Frechen, Bayer AG, Research & Development, Pharmaceuticals, Systems Pharmacology & Medicine, Building B106, 51368 Leverkusen, Germany.

Email: [sebastian.frechen@bayer.com](mailto:sebastian.frechen@bayer.com)

## Present address

André Dallmann, Bayer HealthCare SAS, Loos, France

## Abstract

Vericiguat (Verquvo; US: Merck, other countries: Bayer) is a novel drug for the treatment of chronic heart failure. Preclinical studies have demonstrated that the primary route of metabolism for vericiguat is glucuronidation, mainly catalyzed by uridine diphosphate-glucuronosyltransferase (UGT)1A9 and to a lesser extent UGT1A1. Whereas a drug–drug interaction (DDI) study of the UGT1A9 inhibitor mefenamic acid showed a 20% exposure increase, the effect of UGT1A1 inhibitors has not been assessed clinically. This modeling study describes a physiologically-based pharmacokinetic (PBPK) approach to complement the clinical DDI liability assessment and support prescription labeling. A PBPK model of vericiguat was developed based on in vitro and clinical data, verified against data from the mefenamic acid DDI study, and applied to assess the UGT1A1 DDI liability by running an in silico DDI study with the UGT1A1 inhibitor atazanavir. A minor effect with an area under the plasma concentration–time curve (AUC) ratio of 1.12 and a peak plasma concentration ratio of 1.04 was predicted, which indicates that there is no clinically relevant DDI interaction anticipated. Additionally, the effect of potential genetic polymorphisms of UGT1A1 and UGT1A9 was evaluated, which showed that an average modest increase of up to 1.7-fold in AUC may be expected in the case of concomitantly reduced UGT1A1 and UGT1A9 activity for subpopulations expressing non-wild-type variants for both isoforms. This study is a first cornerstone to qualify the PK-Sim platform for use of UGT-mediated DDI predictions, including PBPK models of perpetrators, such as mefenamic acid and atazanavir, and sensitive UGT substrates, such as dapagliflozin and raltegravir.

This is an open access article under the terms of the [Creative Commons Attribution-NonCommercial](https://creativecommons.org/licenses/by-nc/4.0/) License, which permits use, distribution and reproduction in any medium, provided the original work is properly cited and is not used for commercial purposes.

© 2023 The Authors. *CPT: Pharmacometrics & Systems Pharmacology* published by Wiley Periodicals LLC on behalf of American Society for Clinical Pharmacology and Therapeutics.

## Study Highlights

### WHAT IS THE CURRENT KNOWLEDGE ON THE TOPIC?

CYP-mediated drug–drug interactions (DDIs) are frequently assessed via *in silico* physiologically-based pharmacokinetic (PBPK) studies instead of dedicated clinical studies. However, the use of PBPK to assess UGT-mediated DDI is not well-established. Vericiguat, a novel drug for chronic heart failure, is a UGT1A9 and 1A1 substrate that was tested with the UGT1A9 inhibitor mefenamic acid in a clinical DDI study.

### WHAT QUESTION DID THIS STUDY ADDRESS?

What is the predicted effect of the UGT1A1 inhibitor atazanavir on the PKs of vericiguat using PBPK modeling?

### WHAT DOES THIS STUDY ADD TO OUR KNOWLEDGE?

PBPK models for vericiguat, for the inhibitors mefenamic acid and atazanavir, and the victim compounds dapagliflozin (for UGT1A9) and raltegravir (for UGT1A1), were successfully built and verified. The prospective UGT1A1 DDI simulation results suggest a low potential for vericiguat to be subject to DDI when coadministered with UGT1A1 inhibitors.

### HOW MIGHT THIS CHANGE DRUG DISCOVERY, DEVELOPMENT, AND/OR THERAPEUTICS?

This study lays a cornerstone for the qualification of the Open Systems Pharmacology platform regarding reliable PBPK predictions of UGT-mediated DDIs during model-informed drug development.

## INTRODUCTION

Vericiguat is an orally administered direct soluble guanylate cyclase stimulator that was investigated in the phase III VICTORIA study (NCT02861534) versus placebo in patients with symptomatic chronic heart failure (HF) and left ventricular ejection fraction less than 45% who had been receiving guideline-directed medical therapy and had a previous worsening HF event for which hospitalization or urgent treatment was warranted.<sup>1</sup> In the VICTORIA study, a reduction in the primary composite end point of cardiovascular death or HF hospitalization in patients receiving vericiguat relative to placebo was demonstrated.<sup>1</sup> Vericiguat has been approved in the United States, the European Union, Japan, China, and several other countries under the tradename Verquvo (US: Merck, other countries: Bayer).

Vericiguat exhibits linear pharmacokinetics (PKs), shows a low total plasma clearance of about 1.6 L/h in healthy volunteers, and has an absolute bioavailability of 93% when taken with food.<sup>2</sup> The fraction unbound in plasma is ~2%.<sup>3,4</sup> Vericiguat is a substrate of P-glycoprotein (P-gp) and breast cancer resistance protein (BCRP).<sup>2</sup> Preclinical and clinical studies have demonstrated that the primary route of metabolism for

vericiguat is glucuronidation to an inactive metabolite (M-1; N-glucuronide).<sup>3</sup> Glucuronidation is mainly catalyzed by uridine diphosphate-glucuronosyltransferase (UGT)1A9, as well as 1A1 to a lesser extent.<sup>2,3</sup> Vericiguat is also cleared via other routes, including renal elimination by glomerular filtration, possible excretion of unchanged vericiguat via bile/intestinal secretion, and to a minor extent (<5%), cytochrome P450 (CYP)-mediated oxidative biotransformation.<sup>3</sup> Consequently, clinically significant drug–drug interactions (DDIs) with CYP do not play a role for vericiguat; however, considering the major role of UGT1A9 and UGT1A1 for the clearance of vericiguat, the DDI potential for DDI with UGT inhibitors needs to be assessed.

*In vitro* DDI studies were conducted to assess the effect of known UGT inhibitors on the glucuronidation of vericiguat. Based on this initial *in vitro* DDI risk assessment, an *in vivo* DDI study with the UGT1A9 inhibitor mefenamic acid was conducted.<sup>3</sup> The results showed that pre-administration and co-administration of mefenamic acid (total dose of 3500 mg over 3 days) had a moderate non-clinically relevant influence on the exposure of a single dose of 2.5 mg vericiguat (about 20% increase in the area under the curve [AUC] in healthy adults).<sup>3</sup> The effect of UGT1A1 inhibitors has not been assessed clinically.

Recent guidance documents of the US Food and Drug Administration (FDA)<sup>5</sup> and the European Medicines Agency<sup>6</sup> explicitly promote the use of physiologically-based PK (PBPK) models for the evaluation of the DDI liability for new investigational drugs. PBPK modeling provides a powerful mechanistic framework that integrates drug properties and system-specific organism properties, and has effectively become an integral part of drug development while concepts of ensuring the quality of specialized PBPK software platforms, such as PK-Sim®, and the credibility of PBPK model-based derived conclusions have evolved.<sup>7</sup> Regulatory acceptance is closely linked to the demonstration of predictive capability and accuracy of PBPK platforms in the area of the intended use<sup>8</sup> (i.e., the so-called PBPK platform qualification for an intended purpose). Thus, assessment of CYP-mediated DDIs via in silico PBPK studies in lieu of the dedicated clinical studies represents a frequent application with a long history of success in supporting prescription labeling and submission under certain conditions.<sup>9–14</sup> Nonetheless, the use of PBPK modeling to assess UGT-mediated DDIs is not well-established and only a few examples exist.<sup>15–17</sup> From a modeling perspective, the same principles for CYP-mediated DDIs apply to UGT-mediated DDIs. Therefore, an in silico PBPK approach was considered appropriate to complement the in vivo DDI potential assessment of vericiguat from the clinical DDI study with the UGT1A9 inhibitor mefenamic acid.<sup>3</sup>

Polymorphisms of UGT1A1 and UGT1A9 have been described in multiple ethnicities, with varying allele frequencies leading to different enzyme activities.<sup>18</sup> The current study aimed to derive a quantitative understanding of potential effects of such polymorphisms via PBPK simulations applying a heuristic modeling approach.

Specifically, the goals of this study were:

1. To develop a verified PBPK model of vericiguat and its major inactive metabolite M-1 based on in vitro and clinical PK data that provide a quantitative understanding of the disposition pathways and PKs;
2. to assess the UGT1A1 victim DDI liability of vericiguat by running an in silico DDI study with the known UGT1A1 inhibitor atazanavir in a PBPK platform qualified for this purpose;
3. To evaluate the impact of potential genetic polymorphisms of UGT1A1 and UGT1A9 on the plasma concentrations of vericiguat and M-1; and
4. To qualify the PK-Sim platform for the purpose of UGT-mediated DDI predictions including the effects of perpetrators, such as mefenamic acid and atazanavir on UGT substrates, such as dapagliflozin and raltegravir.

## METHODS

### PBPK modeling and simulation strategy and software

The modeling strategy to assess the in silico DDI liability for vericiguat shown in Figure 1 involved (1) the qualification of the PBPK platform for the intended purpose of simulating UGT-mediated DDIs by first developing PBPK models of the UGT inhibitors mefenamic acid (UGT1A9) and atazanavir (UGT1A1) and the UGT substrates dapagliflozin (UGT1A9) and raltegravir (UGT1A1), and verifying the models with published clinical DDI data; (2) the development; (3) evaluation of a PBPK model for vericiguat and its major metabolite M-1; (4) the verification of the vericiguat PBPK model with regard to its UGT metabolism by utilizing the observed data from the mefenamic acid/vericiguat DDI study, and finally (5), the application of the vericiguat PBPK model to evaluate the UGT1A1 DDI potential in a virtual atazanavir/vericiguat DDI study. All PBPK models were built based on selected clinical data and applicable in vitro data using a middle-out approach.<sup>19</sup> The model reference individuals used were the standard humans implemented in PK-Sim (men: 30years old, 70 kg, 176 cm; women: 30years old, 60 kg, 163 cm).

Vericiguat model evaluation, verification, and application was performed via population simulations. Specifically, a virtual healthy European volunteer population ( $n=1000$ ) was generated based on the specified demographic inclusion criteria of the clinical mefenamic acid/vericiguat DDI study<sup>3</sup>: men, age 18–55years, and body mass index 18–30 kg/m<sup>2</sup>.

The relative tissue-specific expressions of enzymes and transporters being relevant for the respective PBPK models were considered based on high-sensitivity real-time polymerase chain reaction mRNA data (as available in PK-Sim).<sup>20–22</sup> The absolute expressions (so-called *reference concentrations*) were obtained by considering the respective absolute concentration in the liver for UGT1A9 and UGT1A1, as reported by Ohtsuki et al.,<sup>23</sup> for P-gp and BCRP as reported by Tucker et al.,<sup>24</sup> CYP1A1 internal data, and CYP3A4 as reported by Rodriguez et al.<sup>25</sup>

The original PBPK modeling analysis was performed using the Open Systems Pharmacology (OSP) software tools PK-Sim and MoBi (OSP version 8).<sup>26</sup>

### UGT-DDI qualification

The utilization of the PBPK platform PK-Sim in a regulatory context requires its qualification for an intended use. A technical framework for automatic PBPK platform (re-)

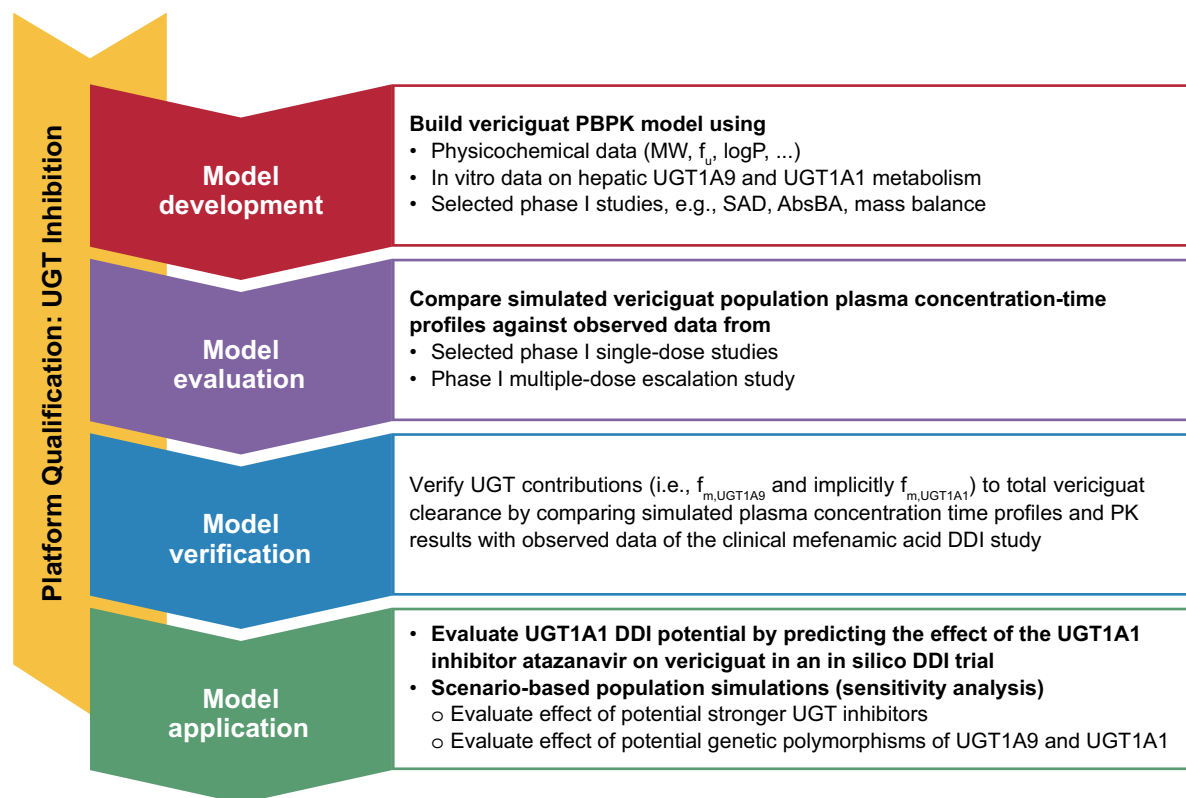


**FIGURE 1** Modeling strategy and workflow of the presented PBPK analysis for vericiguat. AbsBA, absolute bioavailability; DDI, drug–drug interaction;  $f_u$ , fraction unbound in plasma;  $f_m$ , fraction metabolized; logP, octanol–water partition coefficient (lipophilicity); MW, molecular weight; PBPK, physiologically based pharmacokinetics; PK, pharmacokinetics; SAD, single dose ascending; UGT, uridine diphosphate-glucuronosyltransferase.

qualification of PK-Sim was developed to demonstrate the platform's overall capability for a specific intended simulation purpose.<sup>13</sup> The respective software for this framework is freely available on the OSP GitHub site.<sup>27</sup>

To demonstrate the applicability of the platform for the prospective evaluation of UGT-mediated DDIs in the context of reversible inhibition, four PBPK models were built as part of the presented in silico DDI liability assessment of vericiguat. Models for the inhibitors mefenamic acid and atazanavir, featuring reversible UGT1A9 and UGT1A1 inhibition, respectively, were built using publicly available clinical PK data, whereas their respective inhibition parameters were determined in vitro using established probe substrates in recombinant UGT systems in this study (see [Supplementary Material S1](#) section “In vitro experiments”). PBPK models for the UGT substrates dapagliflozin (as a sensitive UGT1A9 substrate) and raltegravir (as a sensitive UGT1A1 substrate) were developed using publicly available data.

Published clinical DDI study data for the interaction between mefenamic acid and dapagliflozin were utilized to verify the capability of the mefenamic acid PBPK model to correctly predict the magnitude of UGT1A9-mediated DDIs.<sup>28</sup> Similarly, the atazanavir PBPK model was verified

utilizing published data from clinical DDI studies with atazanavir and raltegravir.<sup>29–32</sup>

By using the experimental in vitro results for mefenamic acid and atazanavir inhibition as direct model inputs, the platform was deemed qualified with regard to reversible UGT inhibition if the area under the plasma concentration-time curve ratios (AUCRs) were successfully predicted based on the criterion proposed by Guest et al.<sup>33</sup> and an acceptable recovery of the concentration-time profile of the substrates dapagliflozin and raltegravir was demonstrated. The limits for acceptance proposed by Guest et al. converge as the observed ratio reaches 1 and approximate the conventional two-fold boundaries as the ratio increases.

More details on the development and evaluation of the models for mefenamic acid,<sup>34</sup> dapagliflozin,<sup>35</sup> atazanavir,<sup>36</sup> and raltegravir<sup>37</sup> are reported in the OSP GitHub platform under the given references, where the models are publicly available.

## Vericiguat PBPK model development

The base PBPK model to describe the PK of vericiguat and M-1 in plasma, urine, and feces was established using

physicochemical and in vitro input data (Table S1.1), and was additionally informed from observed clinical data from three key clinical pharmacology phase I single-dose studies (i.e., the single-dose escalation study<sup>38</sup> [Table S1.2, A], the mass balance study<sup>3</sup> [Table S1.2, G], and the absolute bioavailability study [EudraCT 2015-001568-20; Table S1.2, K]). Key components of the whole-body coupled PBPK model of vericiguat and M-1 represent glucuronidation of vericiguat to M-1 through UGT1A9 (kidneys and liver) and UGT1A1 (primarily the liver), oxidative metabolism via CYP1A1 and CYP3A4, active transport of vericiguat via P-gp and BCRP, renal tubular and biliary secretion of M-1, and cleavage of M-1 back to vericiguat in the lumen of the large intestine (presumably through beta-glucuronidases of the intestinal microbiota).<sup>39–42</sup>

An integrated analysis of PK data from several clinical studies (including respective mass balance data in urine and feces) informed the following key pathway contributions to the total clearance of vericiguat: (1) the overall glucuronidation to M-1 (from both UGT1A1 and UGT1A9), (2) oxidative metabolism, and (3) excretion of unchanged drug into urine. The split of the total glucuronidation pathway into two specific clearance pathways via UGT1A9 and UGT1A1 in the model was further informed by in vitro studies that determined the relative contributions of UGT1A9 and UGT1A1 to hepatic glucuronidation of vericiguat as being 60% versus 40%, respectively (Table S1.1 and Supplementary Material S1 section “In vitro experiments”). This ratio was used as direct input for the vericiguat PBPK model together with the organ-specific absolute expressions of the two UGT enzymes (Table S1.3 and S1.4) to parametrize the two distinct UGT-mediated clearance pathways in the model. This results in fractions metabolized of total clearance (including extrahepatic components) via UGT1A9 versus UGT1A1 (for details see Supplementary Material S1 section “Supporting documentation PBPK modeling”).

During model development, unknown model parameters of the base model were estimated using the parameter identification module provided in PK-Sim. Additionally, the input parameter lipophilicity of vericiguat was slightly adjusted as a surrogate parameter for partitioning as described in Kuepfer et al.<sup>43</sup> Once the base model was parametrized, additional parameters for the dissolution kinetics of different immediate-release (IR) tablets under fasted and fed conditions were fitted empirically using Weibull functions to a set of additional clinical data (Table S1.2).

Exploratory analysis of clinical data suggested an apparent time-dependent renal clearance of the excretion of M-1 into urine (Figure S1.1). Interestingly, the initial renal clearance of M-1 was greater than the renal clearance expected from the glomerular filtration rate (GFR)

for the unbound fraction in plasma. However, renal clearance of M-1 decreased with time (after dose) and eventually approached the level estimated from only passive elimination via GFR. To describe this phenomenon and using that respective clinical data, an empirical solution was implemented, whereby the permeability of M-1 from the interstitial space into the kidney's cell was estimated.

## Vericiguat PBPK model evaluation

Population simulations with the final PBPK model of vericiguat and M-1 were performed, and the results were compared against observed clinical data from various studies (Table S1.2) to evaluate model appropriateness with regard to describing the PK of vericiguat and M-1.

## Vericiguat PBPK model verification

The PBPK model for vericiguat was first verified with regard to its UGT metabolism by comparing simulated and observed data of the DDI study of vericiguat co-administered with the UGT1A9 inhibitor mefenamic acid.<sup>3</sup> A population simulation was performed applying the study design from the mefenamic acid/vericiguat DDI study<sup>3</sup>: mefenamic acid, 500 mg loading dose, followed by twelve doses of 250 mg mefenamic acid every 6 h; vericiguat, 2.5 mg single dose on day 2 simultaneous with the fifth dose of mefenamic acid (24 h after the first mefenamic acid dose). AUCR and maximum concentration ratios ( $C_{\max}$ Rs) of vericiguat in the presence and absence of mefenamic acid were assessed and compared with observed data. The vericiguat model was deemed verified in the case of a successful simulation based on the criterion proposed by Guest et al.<sup>33</sup> and an acceptable recovery of the concentration-time profile of vericiguat in the presence of mefenamic acid. A summary of the simulation design is listed in Table S1.

## Vericiguat PBPK model application

The verified vericiguat model was then used to evaluate (1) the effect of the UGT1A1 inhibitor atazanavir and (2) the impact of potential genetic polymorphisms of both UGT1A9 and UGT1A1 on the PKs of vericiguat.

Population simulations were performed to assess AUCR and  $C_{\max}$ R of vericiguat in the presence and absence of atazanavir. The atazanavir was administered at a dose of 400 mg once daily over 12 days and a single dose of 10 mg vericiguat was administered on day 7 simultaneously with the seventh dose of atazanavir.

Additionally, sensitivity analysis scenarios were simulated. First, the DDI liability of vericiguat as a victim of its primary clearance pathway UGT1A9 was further characterized in this PBPK study. Mefenamic acid cannot be considered a truly strong UGT1A9 inhibitor given its typical steady state exposure, the low fraction unbound in plasma (~2%),<sup>34</sup> and the respective unbound  $K_i$  value of 0.3  $\mu\text{M}$  (Tables S1.6 and S1.7). Therefore, to account for the potential impact of (hypothetically) stronger UGT1A9 inhibitors, scenario-based population simulations were conducted, assuming varying levels of partial to full (static) inhibition of the UGT1A9 pathway (with reductions by 25%, 50%, 75%, and 100% of the UGT1A9 clearance pathway).

Second, the effect of potential genetic polymorphisms of both UGT1A9 and UGT1A1 on the PKs of vericiguat and M-1 was evaluated similarly in a heuristic approach, applying four different scenarios: scenario 1: reduction of UGT1A1 activity by a factor of 0.5; scenario 2: reduction of UGT1A9 activity by a factor of 0.5; scenario 3: reduction of both UGT1A1 and UGT1A9 activity by a factor of 0.5; and scenario 4: increase of UGT1A9 activity by a factor of 2. These simulation scenarios were chosen based on clinical observations of other UGT1A9 or UGT1A1 substrates in the presence of different genetic variants.<sup>18,44–52</sup> A summary of the simulation design for all model applications is listed in Table S1.5.

Finally, uncertainty in resulting fractions metabolized of UGT1A1 and UGT1A9 in the vericiguat model was assessed in a dedicated sensitivity analysis.

## RESULTS

### UGT-DDI qualification

PBPK models for the inhibitors UGT1A9 mefenamic acid, UGT1A1 atazanavir, and the victim compounds dapagliflozin (for UGT1A9) and raltegravir (for UGT1A1) were successfully built and verified. Both inhibitors, mefenamic acid and atazanavir, demonstrated in vitro inhibition by a mixed-type mechanism. The determined inhibition parameters (Table S1.7) served as direct input for the PBPK models of mefenamic acid and atazanavir without further modification.

The mefenamic acid model was verified regarding UGT1A9 inhibition by utilizing the published clinical DDI study comparing mefenamic acid and the victim drug dapagliflozin.<sup>28</sup> A simulated AUCR of 1.34 in a typical virtual healthy individual was obtained, which slightly underpredicted the observed AUCR of 1.51 by a factor of 0.89.<sup>28</sup> This may be explained by additional inhibition of UGT2B7, which is known to contribute to the metabolism of dapagliflozin.<sup>15</sup> UGT2B7 inhibition was not considered in the simulation owing to a lack of a reliable (in vitro)  $K_i$  value. Nevertheless, the simulated AUCR and  $C_{\text{max}}$  is in the range of the criterion for a successful prediction (Figure 2).

The atazanavir model was also verified regarding UGT1A1 inhibition, using published clinical DDI studies comparing atazanavir and the victim drug raltegravir.<sup>29–32</sup> The simulated AUCRs were all within the criterion for a

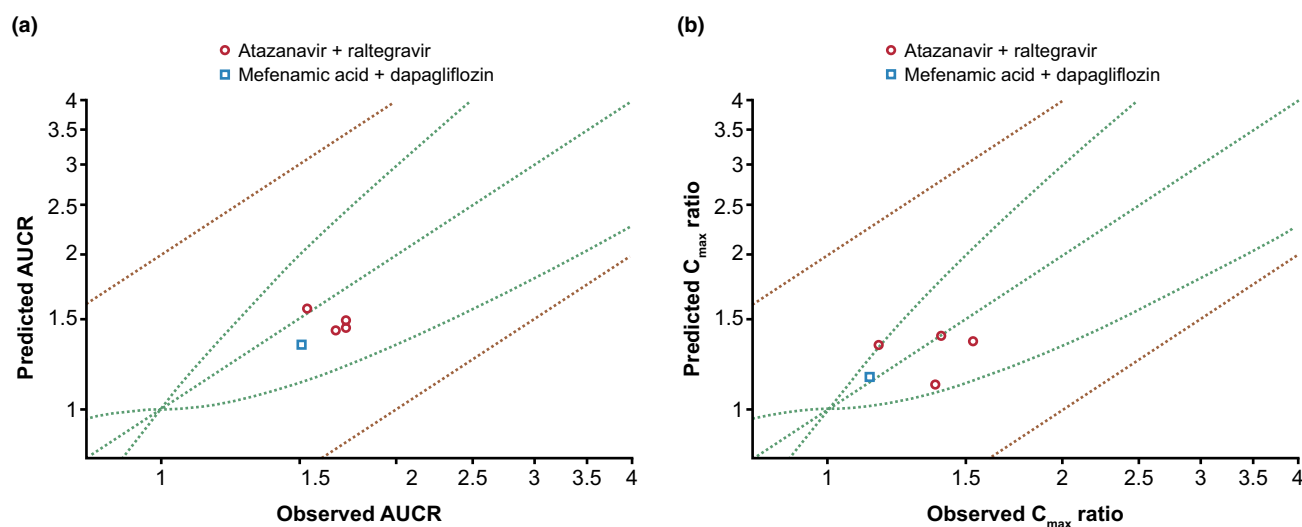


**FIGURE 2** Platform qualification: model verification of UGT1A9-mediated DDI of mefenamic acid and UGT1A1-mediated DDI of atazanavir. Plots from UGT DDI Inhibition Qualification report.<sup>53</sup> (a) Predicted versus observed AUCR; (b) predicted versus observed  $C_{\text{max}}$  ratios. Outer lines denote 0.50–2.00 (two-fold) criterion; inner lines denote the limits as suggested by Guest et al.<sup>33</sup> Clinical studies: mefenamic acid and dapagliflozin,<sup>28</sup> atazanavir and raltegravir.<sup>29–32</sup> AUCR, area under the plasma concentration–time curve;  $C_{\text{max}}$ , maximum concentration; DDI, drug–drug interaction; UGT; uridine diphosphate-glucuronosyltransferase.

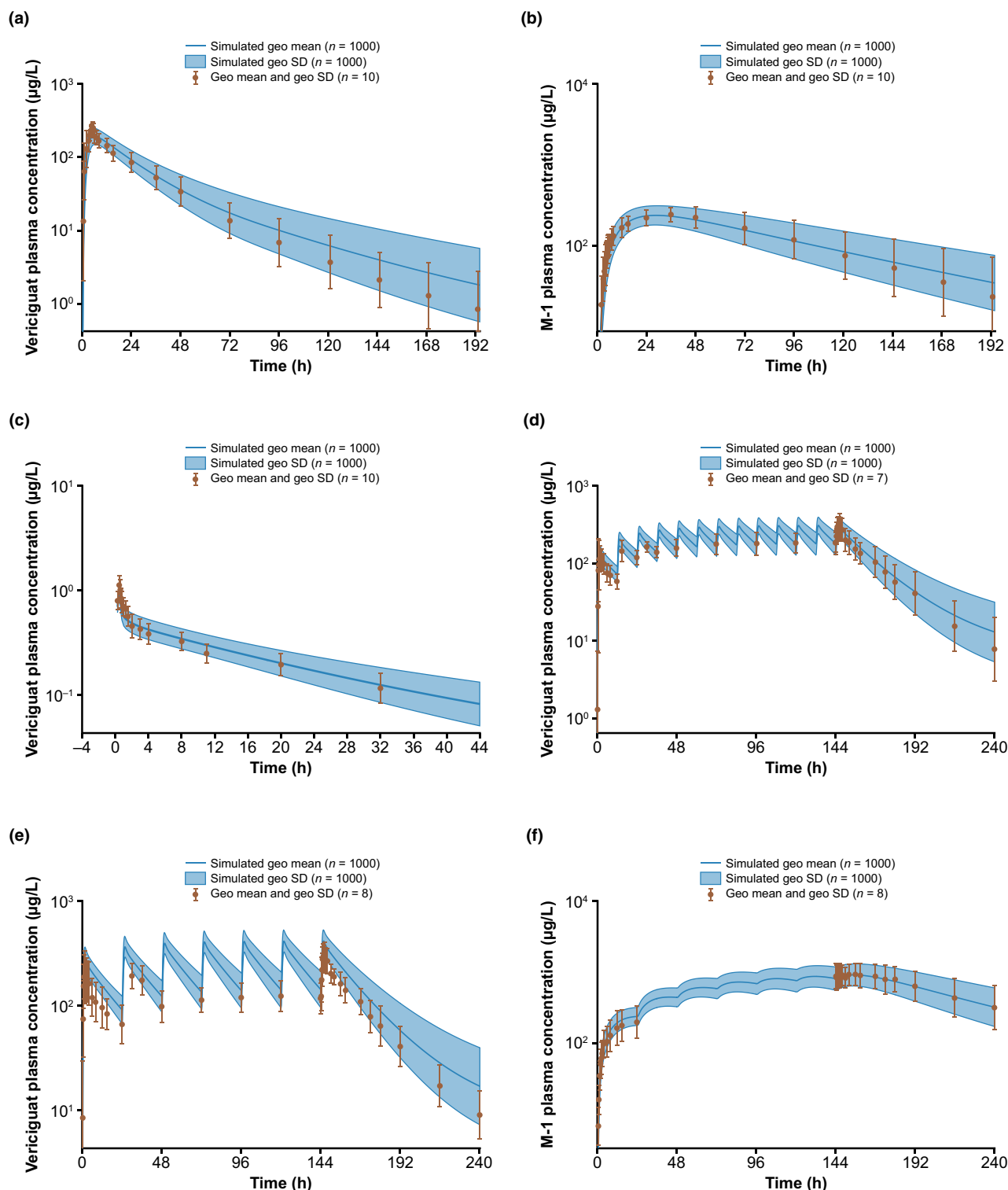


**FIGURE 3** Simulated versus observed time profiles of vericiguat and M-1 plasma concentration for selected clinical studies. (a–c) Observed data are from the absolute bioavailability study (EudraCT 2015-001568-20). (d–f) Observed data from the multiple dose escalation study.<sup>38</sup> (a, b) Plasma concentration of vericiguat and M-1 after single doses of 10 mg vericiguat orally. (c) Vericiguat plasma concentration after 0.02 mg of vericiguat administered intravenously. (d) Vericiguat plasma concentration after 5 mg of vericiguat given twice daily. (e, f) Vericiguat and M-1 plasma concentration after 10 mg vericiguat given once daily. Observed data: dots represent geometric mean, whiskers represent geometric standard deviation. Statistics at any timepoint were only calculated if at least two-thirds of the individual data were measured and were above the LLOQ. For their calculation a data point below the LLOQ was substituted by one-half of this limit. Simulated data: solid lines represent geometric mean, shaded areas represent fifth to ninth population prediction interval. Geo., geometric; LLOQ, lower limit of quantification; SD, standard deviation.

successful prediction (Figure 2). Although three of the four simulations showed a slight underprediction<sup>29–31</sup> and one simulation showed a minor overprediction,<sup>32</sup> the corresponding overall geometric mean fold error over the four simulations, 1.13, was low.

With the direct success in the good recovery of observed clinical DDI studies both for mefenamic acid and atazanavir using the measured in vitro inhibition parameters, the PBPK platform was considered qualified for the use of simulating reversible inhibition of UGTs. Further details on the evaluation of the DDI studies can be found in the publicly available qualification report on the OSP GitHub platform.<sup>53</sup>

### Vericiguat PBPK model description and evaluation

An overview of all drug-specific parameters of the final vericiguat/M-1 model is summarized in Table S1.8. Further details are shown in Figure S1.1 and the Supplementary Material S1 section “Supporting documentation PBPK modeling.”

The PBPK model of vericiguat and its metabolite M-1 in adults provides an adequate description of the observed PK data in plasma, urine, and feces for different types of administration (oral solution, IR tablets, and intravenous infusion), over a dose range of 0.5–15 mg, as well as for administration of vericiguat as single and multiple doses under fasted and fed state conditions. Exemplarily, simulated concentration-time profiles of a virtual healthy population compared with observed data for the absolute bioavailability study (EudraCT 2015-001568-20, part of the model-building dataset), after single doses of 10 mg orally and 0.02 mg intravenously, and for the multiple-dose escalation study (not part of the model-building dataset) after 10 mg once daily and 5 mg twice daily<sup>38</sup> are shown in

Figure 3. Further detailed time profile plots can be found in Figure S1.2.

Based on the final PBPK model, simulations showed that 43% of the orally administered vericiguat dose is excreted unchanged to feces, 41% is excreted as M-1 into urine via tubular secretion and glomerular filtration, 9% is excreted unchanged into urine (mainly via glomerular filtration), and 6% is oxidatively metabolized, whereas no significant amount of M-1 is excreted into feces. These results are in excellent agreement with respective data from the mass balance study (Figure 4).<sup>3</sup> Considering the absolute bioavailability of vericiguat of more than 90% and the results of a univariate sensitivity analysis (data not shown), the model suggests that the major part of the ~40% unchanged vericiguat in feces results from the assumed cleavage of the glucuronic acid in the lumen of the large intestine. This results in conversion of the biliary-secreted M-1 to its parent, whereas the model suggests a rather limited role of the efflux transporters (i.e., P-gp/BCRP) for vericiguat's PKs. Drawing from preliminary explorations utilizing the PBPK model, it appears that the role of transporters is primarily in restricting the colonic re-absorption of cleaved molecules.

Based on the model, after a 10 mg oral dose of vericiguat, the fraction metabolized (of whole-body total clearance) via UGT1A9 is ~67% and the fraction metabolized via UGT1A1 is ~19% (Figure 5).

### Vericiguat PBPK model verification

The PBPK model adequately simulated the observed DDIs between mefenamic acid and vericiguat from the clinical DDI study,<sup>3</sup> with an observed AUCR of 1.20 versus a simulated AUCR of 1.14, and an observed  $C_{\max}$ R of 0.97 versus a simulated  $C_{\max}$ R of 1.06 (Table 1). Correspondingly, simulated concentration-time profiles of vericiguat and

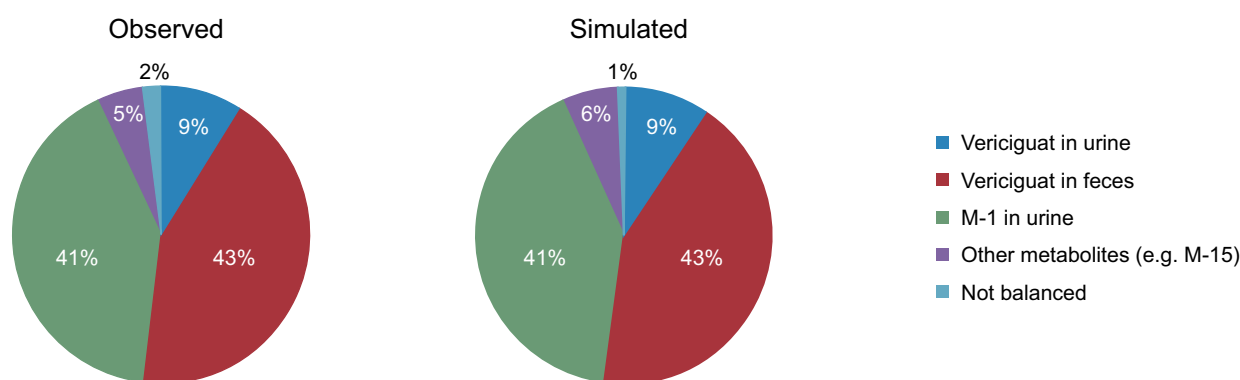


**FIGURE 4** Mass balance of vericiguat observed versus simulated. Observed data from a clinical mass balance study.<sup>3</sup> The 320 h were simulated. Percentages indicate the amounts excreted into the respective compartments. Excretion of M-1 into feces was less than 0.1%. The fraction “other metabolites” in the observed pie refers to the summed amounts of metabolites other than M-1 excreted to urine and feces.

mefenamic acid were well in line with the respective observed data (Figure 6). Thus, the fraction metabolized via UGT1A9 (and thus implicitly the fraction metabolized via UGT1A1) in the vericiguat PBPK model was deemed verified for use in prospective PBPK evaluations in the context of UGT-mediated DDIs.

## Vericiguat PBPK model application

The prospective simulation of a virtual DDI study between the UGT1A1 inhibitor atazanavir and vericiguat predicted an AUCR of 1.12 and a  $C_{\max}$ R of 1.04 (Table 1).

The results of the sensitivity analysis scenarios to quantify the potential impact of (hypothetically) stronger UGT1A9 inhibitors showed that a potential worst-case scenario featuring complete inhibition of the UGT1A9 pathway in the vericiguat PBPK model would lead on average to a 3.1-fold increase in vericiguat exposure.

The assessment of potential UGT1A1 and/or UGT1A9 polymorphisms indicated that in such subpopulations, the AUC may vary on average between 0.6- to 1.7-fold compared with the exposure expected in the total population.

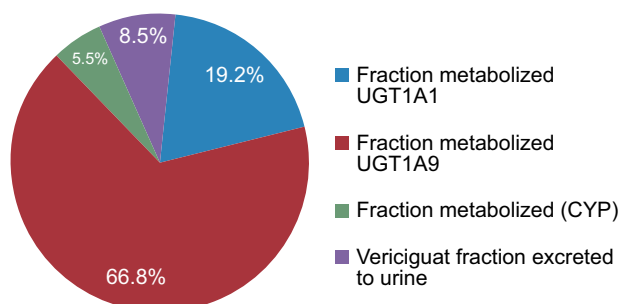


**FIGURE 5** Clearance pathway contributions in the final PBPK model of vericiguat and M-1. CYP, cytochrome P450; PBPK, physiologically based pharmacokinetics; UGT, uridine diphosphate-glucuronosyltransferase.

Details on the results of the sensitivity analysis scenarios are outlined in Table 2.

The uncertainty assessment via a dedicated sensitivity analysis on the fractions metabolized via UGT1A1 and UGT1A9 revealed that a realistic and justifiable range for the fraction metabolized of UGT1A9 is from 56% to 78% (see Supplementary Material S2 “Sensitivity Analysis on Fractions metabolized of UGT1A1 and UGT1A9”). The corresponding fraction metabolized of UGT1A1 then ranges from 7.5% to 30% resulting in respective mean AUCR increases from 1.06 to 1.17.

## DISCUSSION

PBPK provides a powerful framework to integrate drug and system-specific organism properties.<sup>7,11</sup> The PBPK model established for vericiguat and M-1 integrated physicochemical, in vitro, and clinical data, have provided a quantitative understanding of the disposition pathways and PK in healthy adults. Specifically, a more detailed comprehension of the glucuronidation process as the major clearance/excretion pathway for vericiguat was established.<sup>3</sup>

In this study, PBPK modeling was used to assess UGT-mediated DDIs. In a dedicated clinical pharmacology study, mefenamic acid, a UGT1A1 inhibitor, was shown to increase vericiguat concentrations, but the effect size was deemed to be not clinically meaningful. The PBPK model of vericiguat described here extends this finding such that no further corresponding clinical DDI study is required to evaluate the effects of either UGT1A9 or UGT1A1 inhibition on vericiguat as a victim.

Although PBPK modeling has been frequently and successfully applied in the area of CYP-mediated DDI risk assessment and a decent set of qualification packages now exists for this purpose,<sup>12,13,54</sup> there has been no such

**TABLE 1** Simulated/predicted and observed AUCR and  $C_{\max}$ R of vericiguat following co-administration of mefenamic acid and atazanavir.

Inhibitor	AUCR	$C_{\max}$ R
Mefenamic acid		
Simulated	1.14 (5.3%) <sup>a</sup> [1.06, 1.25] <sup>b</sup>	1.06 (6.0%) <sup>a</sup> [1.01, 1.20] <sup>b</sup>
Observed	1.20 (8.3%) <sup>a</sup> [1.13, 1.27] <sup>c</sup>	0.97 (9.6%) <sup>a</sup> [0.90, 1.03] <sup>c</sup>
Simulated/observed ratio	0.95	1.09
Atazanavir		
Predicted	1.12 (2.9%) <sup>a</sup> [1.07, 1.17] <sup>c</sup>	1.04 (1.1%) <sup>a</sup> [1.03, 1.06] <sup>c</sup>

Abbreviations: AUCR, area under the plasma concentration–time curve ratio;  $C_{\max}$ R, maximum concentration ratio; CV, coefficient of variation.

<sup>a</sup>Geometric mean (%CV).

<sup>b</sup>The 90% confidence interval around the observed geometric mean ratio.

<sup>c</sup>The 90% population interval due to population variability.

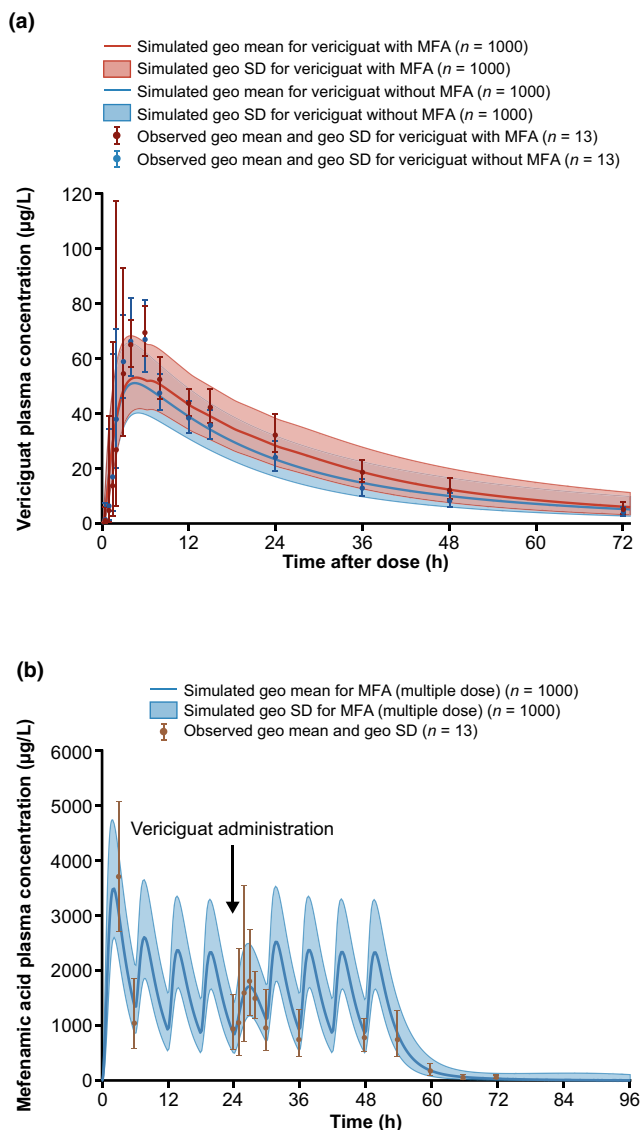


**FIGURE 6** Simulation of the UGT1A9-mediated DDI between mefenamic acid and vericiguat. Observed data: from the mefenamic acid DDI study<sup>3</sup> (in both panels); dots represent geometric mean, whiskers represent geometric standard deviation. Statistics at any timepoint were only calculated if at least two-thirds of the individual data were measured and were above the lower limit of quantification (LLOQ). For their calculation a data point below the LLOQ was substituted by one half of this limit. Simulated data: solid lines represent geometric mean, shaded areas represent fifth to ninth population prediction interval. DDI, drug–drug interaction; geo., geometric; MFA, mefenamic acid; SD, standard deviation; UGT, uridine diphosphate-glucuronosyltransferase.

qualification reported in the context of UGT-mediated DDI simulations. One essential first step in this *in silico* DDI liability assessment of vericiguat was the successful qualification of the PK-Sim platform for the given purpose of predicting UGT1A1- and UGT1A9-mediated DDIs. Four additional PBPK models of known UGT inhibitors and substrates were independently developed and

verified: mefenamic acid, atazanavir, dapagliflozin, and raltegravir. Remarkably, experimentally determined (unbound) *in vitro* inhibition parameters from recombinant UGT systems using established probe substrates (propofol for UGT1A9 inhibition of mefenamic acid and 17 $\beta$ -estradiol for UGT1A1 inhibition of atazanavir) could be used directly as input parameters in an *in vitro-in vivo* extrapolation approach. Without scaling or fitting these inhibition parameters, DDI simulations could be performed for mefenamic acid with dapagliflozin as victim drug and for atazanavir with raltegravir as victim drug. The applicability of the presented approach was demonstrated by the fact that the simulated AUCR and  $C_{\max}$ R were within the predefined criterion for a successful prediction<sup>33</sup> compared with observed data obtained from published clinical studies.<sup>28–32</sup>

Based on the preceding *in vitro* UGT relative activity factor and chemical inhibition studies, the relative contribution of UGT1A9 versus UGT1A1 to the overall glucuronidation in the liver was estimated to be 60% versus 40% (see [Supplementary Material S1](#) section “Estimation of the UGT1A1 and UGT1A9 contribution to glucuronidation of vericiguat in liver,” “Supporting documentation PBPK modeling,” and [Table S1.1](#)). UGTs are expressed in multiple organs—mainly the liver, kidneys, and gastrointestinal tract—and total metabolism is dependent on the specific UGT isoform expressed in each tissue (e.g., UGT1A9 shows an even higher expression in the kidneys compared with the liver,<sup>22</sup> whereas UGT1A1 is mainly expressed in the liver and to a lower extent in the gastrointestinal tract.)<sup>22</sup> By considering the whole-body expressions and corresponding relative contributions of hepatic versus extrahepatic metabolism in the PBPK model, the respective fractions metabolized of the total clearance of vericiguat could be estimated (i.e., 67% for UGT1A9 and 19% for UGT1A1; [Figure 5](#)). The contribution of UGT1A9 in the model was successfully verified by recovering the clinical DDI data of the mefenamic acid/vericiguat study.<sup>3</sup> With a verification of the UGT1A9 fraction and considering that the model satisfactorily describes the PK of vericiguat and M-1 in plasma, urine, and feces, the UGT1A1 contribution was considered verified as well. The PBPK model of vericiguat was considered verified and suitable for prospective predictions to support and guide the decision making processes in the further development of vericiguat, particularly in the area of DDI risk assessment and exposure prediction in pediatric populations.

In the current study, the performed virtual trial simulation complemented the DDI-liability assessment of vericiguat as a potential victim of UGT-mediated DDIs. Under the co-administration of the UGT1A1 inhibitor atazanavir, the PBPK model predicted a geometric mean

**TABLE 2** Statistics of AUCR and  $C_{\max}$ R of vericiguat and M-1 in sensitivity analysis scenarios.

Sensitivity analysis scenario	Vericiguat		M-1	
	AUCR	$C_{\max}$ R	AUCR	$C_{\max}$ R
Inhibition of UGT1A9				
25%	1.20	1.03	0.96	0.89
50%	1.51	1.06	0.91	0.75
75%	2.04	1.10	0.81	0.57
100%	3.13	1.14	0.61	0.33
Polymorphism scenarios <sup>a</sup>				
Scenario 1	1.08	1.02	0.97	0.96
Scenario 2	1.51	1.06	0.91	0.75
Scenario 3	1.71	1.09	0.85	0.68
Scenario 4	0.60	0.90	1.08	1.30

Note: Values are given as population medians.

Abbreviations: AUCR, area under the plasma concentration–time curve;  $C_{\max}$ R, maximum concentration ratio; UGT, uridine diphosphate-glucuronosyltransferase.

<sup>a</sup>Scenario 1: UGT1A1 reduced by a factor of 0.5; scenario 2: UGT1A9 activity reduced by a factor of 0.5; scenario 3: UGT1A1 and UGT1A9 activity reduced by a factor of 0.5; and scenario 4: UGT1A9 activity increased by a factor of 2.

AUCR of 1.12 and  $C_{\max}$ R of 1.04 with low population variability. The predicted effect lies within the default no-effect boundaries of 0.80–1.25 according to current FDA DDI guidelines,<sup>5</sup> indicating that there is no clinically significant DDI interaction anticipated following coadministration of UGT1A1 inhibitors with vericiguat. The projected minor effect of atazanavir on vericiguat PK is in line with the knowledge that UGT1A1 contributes less to the overall glucuronidation of vericiguat compared with UGT1A9, based on in vitro data,<sup>3</sup> and is consistent with the fact that vericiguat is cleared via multiple routes.

During drug development, the vericiguat PBPK model was continuously updated when relevant clinical data became available, for example, from food effect studies, mass balance studies, DDI studies, etc. Simulation studies during early development informed the design of subsequent clinical studies and paved the path toward the in silico DDI study presented in this paper. The predicted lack of a clinically significant DDI with atazanavir justified that a dedicated clinical DDI study with a UGT1A1 inhibitor was not necessary. The PBPK modeling results were shared with regulatory agencies and, for example, were included in the prescription labeling in the United States informing clinicians that no clinically significant differences on vericiguat PKs were predicted with coadministration of the UGT1A1 inhibitor atazanavir.<sup>2</sup>

In addition to the UGT1A1 DDI assessment, the victim properties of vericiguat toward UGT1A9 were evaluated, as mefenamic acid cannot be considered as a strong UGT1A9 inhibitor, owing to its typical steady-state exposure, the low fraction unbound in plasma of ~2%,<sup>34</sup> and

the respective unbound  $K_i$  value of 0.3  $\mu$ M (Table S1.7). Thus, the results from the clinical trial between mefenamic acid and vericiguat should not be simply extrapolated to other UGT1A9 inhibitors. In this study, the impact of hypothetically stronger UGT1A9 inhibitors (compared with mefenamic acid) on the PKs of vericiguat and M-1 were evaluated by a scenario-based sensitivity analysis. The worst-case scenario with complete UGT1A9 inhibition showed a median AUCR increase by 3.1-fold and a marginal median  $C_{\max}$ R increase of 1.1-fold. This AUC increase is plausible considering an estimated fraction metabolized via UGT1A9 of 67%. However, given that such clinically strong UGT1A9 inhibitors have not yet been identified, to the best of our knowledge, the chance of a complete inhibition in clinical practice is considered rather unlikely. As there is also no acknowledged strong inhibitor of both UGT1A9 and 1A1, we could not mimic a realistic clinically feasible scenario in an in silico study to evaluate the maximum impact of UGT inhibition. It should be noted that among the marketed drugs inhibiting UGT1A9, mefenamic acid seems to be the strongest one.<sup>55,56</sup>

UGT1A1 and UGT1A9 have known polymorphisms affecting their respective activities,<sup>18</sup> which was one additional aspect that was investigated in this study. Although the genetic polymorphisms of UGT1A1 and UGT1A9 were not expected to affect the PKs of vericiguat and M-1 to a clinically relevant extent, given that the overall interindividual variability of the PK of vericiguat was found to be low to moderate throughout the vericiguat program,<sup>3,57</sup> this study intended to provide a quantitative idea of such genetic polymorphisms in a

scenario-based fashion. In general, changes in respective UGT activities led to more pronounced effects on AUC compared with the minor changes in  $C_{\max}$  for vericiguat. The evaluation showed that an average increase of up to 1.7-fold in AUC is hypothetically possible in the case of concomitantly reduced UGT1A1 and reduced UGT1A9 activity (i.e., for subpopulations expressing low activity variants for both isoforms).

Despite the successful verification and the plausibility of the PBPK model considering the good description of clinical data, limitations for applications outside the verified use need to be considered. For example, the empirical implementation/parameterization of the efflux transporters, the reduction of the interstitial to intracellular permeability in the kidneys for M-1 to describe the apparent time-dependent renal clearance of M-1 (as further explained in the [Supplementary Material S1](#) section “Supporting documentation PBPK modeling”), and the dissolution kinetics are the assumptions implemented for fitting the model to available clinical data. In addition, we appreciate that the determination of the fraction metabolized is associated with uncertainty. Still, propagating the associated uncertainty does not change the overall conclusions of this study, in particular that the overall DDI potential with regard to UGT1A1 is very low.

Obviously, the PBPK platform qualification package for UGT-mediated DDIs presented here currently consists of a very limited number of compounds compared with well-established qualification packages for CYP-mediated enzymes of various PBPK platforms.<sup>12,13</sup> However, it provides the first cornerstone for the general qualification of PK-Sim regarding reliable PBPK UGT-mediated DDI predictions. With future addition of further UGT victim drugs and drug combinations, and the establishment of a DDI network of PBPK models with the aid of the already established generic technical framework for platform qualification of PK-Sim,<sup>13</sup> confidence in the predictive capabilities of PBPK modeling for UGT-mediated DDI will also grow.

In summary, considering the results of the clinical DDI study, the results of this PBPK analysis, and the multi-pathway clearance of vericiguat, the probability of vericiguat being a victim of metabolic DDIs in the clinical setting is low. Based on the observed overall safety and tolerability profile of vericiguat across various phase I–III clinical studies,<sup>1,3,4,38</sup> the outcomes from the different PBPK model simulations support no dose adjustment for vericiguat.

## AUTHOR CONTRIBUTIONS

S.F., M.M., N.A.J., C.B., M.L., A.D., S.X., M.E.T., and M.G. wrote the manuscript. S.F., M.M., N.A.J., C.B., S.X., and R.B. designed the research. S.F., M.M., N.A.J., C.B., I.I., A.D., and R.B. performed the research. S.F., M.M., N.A.J., C.B., I.I., A.D., S.X., and M.E.T. analyzed the data.

## ACKNOWLEDGMENTS

Editorial support, including writing, data checking, figure preparation, formatting, proofreading, and submission, was provided by Nadia Rafei and Tina Allen of Scion, London, UK, according to Good Publication Practice (GPP) guidelines, and funded by Bayer AG.

## FUNDING INFORMATION

This work was supported by Bayer AG, Leverkusen, Germany.

## CONFLICT OF INTEREST STATEMENT

S.F., I.I., A.D., M.G., N.A.J., C.B., M.L., R.B., and M.M. are employees and potential stockholders of Bayer AG and may own stock in the company. M.E.T. and S.X. are employees of Merck Sharp & Dohme LLC, a subsidiary of Merck & Co., Inc., Rahway, NJ, USA, and may own stock and/or stock options in Merck & Co., Inc., Rahway, NJ, USA.

## ORCID

Sebastian Frechen  <https://orcid.org/0000-0003-1170-9392>

André Dallmann  <https://orcid.org/0000-0003-1108-5719>

Michael Gerisch  <https://orcid.org/0000-0003-3807-9036>

Rolf Burghaus  <https://orcid.org/0000-0001-7843-427X>

## REFERENCES

1. Armstrong PW, Pieske B, Anstrom KJ, et al. Vericiguat in patients with heart failure and reduced ejection fraction. *N Engl J Med*. 2020;382:1883–1893.
2. Food and Drug Administration. VERQUVO prescribing information. 2021. Accessed February 8, 2021. [https://www.accessdata.fda.gov/drugsatfda\\_docs/label/2021/214377s000lbl.pdf](https://www.accessdata.fda.gov/drugsatfda_docs/label/2021/214377s000lbl.pdf)
3. Boettcher M, Gerisch M, Lobmeyer M, et al. Metabolism and pharmacokinetic drug-drug interaction profile of vericiguat, a soluble guanylate cyclase stimulator: results from preclinical and phase I healthy volunteer studies. *Clin Pharmacokinet*. 2020;59:1407–1418.
4. Boettcher M, Loewen S, Gerrits M, Becker C. Pharmacodynamic and pharmacokinetic interaction profile of vericiguat: results from three randomized phase I studies in healthy volunteers. *Clin Pharmacokinet*. 2021;60:337–351.
5. Food and Drug Administration. In vitro drug interaction studies — cytochrome P450 enzyme- and transporter-mediated drug interactions guidance for industry. 2020 Accessed July 4, 2022. <https://www.fda.gov/regulatory-information/search-fda-guidance-documents/vitro-drug-interaction-studies-cytochrome-p450-enzyme-and-transporter-mediated-drug-interactions>
6. European Medicines Agency. Guideline on the investigation of drug interactions - Revision 1. 2015 Accessed July 4, 2022. <https://www.ema.europa.eu/en/investigation-drug-interactions>
7. Frechen S, Rostami-Hodjegan A. Quality assurance of PBPK modeling platforms and guidance on building, evaluating, verifying and applying PBPK models prudently under the umbrella

- of qualification: why, when, what, how and by whom? *Pharm Res.* 2022;39:1733-1748.
8. European Medicines Agency. Physiologically based pharmacokinetic analyses—format and content guidance for industry. 2022 Accessed July 1, 2022. <https://www.ema.europa.eu/en/reporting-physiologically-based-pharmacokinetic-pbpb-modeling-simulation>
  9. Grimstein M, Yang Y, Zhang X, et al. Physiologically based pharmacokinetic modeling in regulatory science: an update from the U.S. Food and Drug Administration's Office of Clinical Pharmacology. *J Pharm Sci.* 2019;108:21-25.
  10. Luzon E, Blake K, Cole S, Nordmark A, Versantvoort C, Berglund EG. Physiologically based pharmacokinetic modeling in regulatory decision-making at the European medicines agency. *Clin Pharmacol Ther.* 2017;102:98-105.
  11. Zhang X, Yang Y, Grimstein M, et al. Application of PBPK modeling and simulation for regulatory decision making and its impact on US prescribing information: an update on the 2018-2019 submissions to the US FDA's office of clinical pharmacology. *J Clin Pharmacol.* 2020;60(Suppl 1):S160-S178.
  12. Kilford PJ, Chen KF, Crewe K, et al. Prediction of CYP-mediated DDIs involving inhibition: approaches to address the requirements for system qualification of the Simcyp simulator. *CPT Pharmacometrics Syst Pharmacol.* 2022;11:822-832.
  13. Frechen S, Solodenko J, Wendl T, et al. A generic framework for the physiologically-based pharmacokinetic platform qualification of PK-Sim and its application to predicting cytochrome P450 3A4-mediated drug-drug interactions. *CPT Pharmacometrics Syst Pharmacol.* 2021;10:633-644.
  14. International Council for Harmonisation of Technical Requirements for Pharmaceuticals for Human Use (ICH). Drug interaction studies M12. 2022 Accessed December 7, 2022. [https://database.ich.org/sites/default/files/M12\\_Step1\\_draft\\_Guideline\\_2022\\_0524.pdf](https://database.ich.org/sites/default/files/M12_Step1_draft_Guideline_2022_0524.pdf)
  15. Callegari E, Lin J, Tse S, Goosen TC, Sahasrabudhe V. Physiologically-based pharmacokinetic modeling of the drug-drug interaction of the UGT substrate ertugliflozin following co-administration with the UGT inhibitor mefenamic acid. *CPT Pharmacometrics Syst Pharmacol.* 2021;10:127-136.
  16. Konishi K, Minematsu T, Nagasaka Y, Tabata K. Physiologically-based pharmacokinetic modeling for mirabegron: a multi-elimination pathway mediated by cytochrome P450 3A4, uridine 5'-diphosphate-glucuronosyltransferase 2B7, and butyrylcholinesterase. *Xenobiotica.* 2019;49:912-921.
  17. Conner TM, Nikolian VC, Georgoff PE, et al. Physiologically based pharmacokinetic modeling of disposition and drug-drug interactions for valproic acid and divalproex. *Eur J Pharm Sci.* 2018;111:465-481.
  18. Stingl JC, Bartels H, Viviani R, Lehmann ML, Brockmüller J. Relevance of UDP-glucuronosyltransferase polymorphisms for drug dosing: a quantitative systematic review. *Pharmacol Ther.* 2014;141:92-116.
  19. Shebley M, Sandhu P, Emami Riedmaier A, et al. Physiologically based pharmacokinetic model qualification and reporting procedures for regulatory submissions: a consortium perspective. *Clin Pharmacol Ther.* 2018;104:88-110.
  20. Nishimura M, Yaguti H, Yoshitsugu H, Naito S, Satoh T. Tissue distribution of mRNA expression of human cytochrome P450 isoforms assessed by high-sensitivity real-time reverse transcription PCR. *Yakugaku Zasshi.* 2003;123:369-375.
  21. Nishimura M, Naito S. Tissue-specific mRNA expression profiles of human ATP-binding cassette and solute carrier transporter superfamilies. *Drug Metab Pharmacokinet.* 2005;20:452-477.
  22. Nishimura M, Naito S. Tissue-specific mRNA expression profiles of human phase I metabolizing enzymes except for cytochrome P450 and phase II metabolizing enzymes. *Drug Metab Pharmacokinet.* 2006;21:357-374.
  23. Ohtsuki S, Schaefer O, Kawakami H, et al. Simultaneous absolute protein quantification of transporters, cytochromes P450, and UDP-glucuronosyltransferases as a novel approach for the characterization of individual human liver: comparison with mRNA levels and activities. *Drug Metab Dispos.* 2012;40:83-92.
  24. Tucker TG, Milne AM, Fournel-Gigleux S, Fenner KS, Coughtrie MW. Absolute immunoquantification of the expression of ABC transporters P-glycoprotein, breast cancer resistance protein and multidrug resistance-associated protein 2 in human liver and duodenum. *Biochem Pharmacol.* 2012;83:279-285.
  25. Rodríguez-Antona C, Donato MT, Pareja E, Gómez-Lechón MJ, Castell JV. Cytochrome P-450 mRNA expression in human liver and its relationship with enzyme activity. *Arch Biochem Biophys.* 2001;393:308-315.
  26. Open Systems Pharmacology. PK-SIM® and MOBI® for PBPK and quantitative systems pharmacology. Accessed July 4, 2022. <https://www.open-systems-pharmacology.org/>
  27. Open Systems Pharmacology. Release of OSP qualification framework. Accessed December 18, 2020. <https://github.com/Open-Systems-Pharmacology/QualificationPlan/releases>
  28. Kasichayanula S, Liu X, Griffen SC, Lacrete FP, Boulton DW. Effects of rifampin and mefenamic acid on the pharmacokinetics and pharmacodynamics of dapagliflozin. *Diabetes Obes Metab.* 2013;15:280-283.
  29. Iwamoto M, Wenning LA, Mistry GC, et al. Atazanavir modestly increases plasma levels of raltegravir in healthy subjects. *Clin Infect Dis.* 2008;47:137-140.
  30. Krishna R, East L, Larson P, et al. Atazanavir increases the plasma concentrations of 1200 mg raltegravir dose. *Biopharm Drug Dispos.* 2016;37:533-541.
  31. Neely M, Decosterd L, Fayet A, et al. Pharmacokinetics and pharmacogenomics of once-daily raltegravir and atazanavir in healthy volunteers. *Antimicrob Agents Chemother.* 2010;54:4619-4625.
  32. Zhu L, Butters J, Persson A, et al. Pharmacokinetics and safety of twice-daily atazanavir 300 mg and raltegravir 400 mg in healthy individuals. *Antivir Ther.* 2010;15:1107-1114.
  33. Guest EJ, Aarons L, Houston JB, Rostami-Hodjegan A, Galetin A. Critique of the two-fold measure of prediction success for ratios: application for the assessment of drug-drug interactions. *Drug Metab Dispos.* 2011;39:170-173.
  34. Frechen S. Building and evaluation of a PBPK model for mefenamic acid in adults. 2020 Accessed July 4, 2022. <https://github.com/Open-Systems-Pharmacology/Mefenamic-acid-Model/releases/tag/v1.0>
  35. Frechen S. Building and evaluation of a PBPK Model for dapagliflozin in adults. 2020 Accessed July 4, 2022. <https://github.com/Open-Systems-Pharmacology/Dapagliflozin-Model/releases/tag/v1.0>

36. Dallmann A. Building and evaluation of a PBPK model for atazanavir in healthy adults. 2020 Accessed July 4, 2022. <https://github.com/Open-Systems-Pharmacology/Atazanavir-Model/releases/tag/v1.0>
37. Ince I. Building and evaluation of a PBPK model for raltegravir in adults. 2020 Accessed July 4, 2022. <https://github.com/Open-Systems-Pharmacology/Raltegravir-Model/releases/tag/v1.0>
38. Boettcher M, Thomas D, Mueck W, et al. Safety, pharmacodynamic, and pharmacokinetic characterization of vericiguat: results from six phase I studies in healthy subjects. *Eur J Clin Pharmacol*. 2021;77:527-537.
39. Blaut M. Ecology and physiology of the intestinal tract. *Curr Top Microbiol Immunol*. 2013;358:247-272.
40. Molly K, Vande Woestyne M, Verstraete W. Development of a 5-step multi-chamber reactor as a simulation of the human intestinal microbial ecosystem. *Appl Microbiol Biotechnol*. 1993;39:254-258.
41. Possemiers S, Verthé K, Uyttendaele S, Verstraete W. PCR-DGGE-based quantification of stability of the microbial community in a simulator of the human intestinal microbial ecosystem. *FEMS Microbiol Ecol*. 2004;49:495-507.
42. Sakamoto H, Yokota H, Kibe R, Sayama Y, Yuasa A. Excretion of bisphenol A-glucuronide into the small intestine and deconjugation in the cecum of the rat. *Biochim Biophys Acta*. 2002;1573:171-176.
43. Kuepfer L, Niederalst C, Wendl T, et al. Applied concepts in PBPK modeling: how to build a PBPK/PD model. *CPT Pharmacometrics Syst Pharmacol*. 2016;5:516-531.
44. Wenning LA, Petry AS, Kost JT, et al. Pharmacokinetics of raltegravir in individuals with UGT1A1 polymorphisms. *Clin Pharmacol Ther*. 2009;85:623-627.
45. Satoh T, Ura T, Yamada Y, et al. Genotype-directed, dose-finding study of irinotecan in cancer patients with UGT1A1\*28 and/or UGT1A1\*6 polymorphisms. *Cancer Sci*. 2011;102:1868-1873.
46. Satoh S, Tada H, Murakami M, et al. Circadian pharmacokinetics of mycophenolic acid and implication of genetic polymorphisms for early clinical events in renal transplant recipients. *Transplantation*. 2006;82:486-493.
47. Cecchin E, Innocenti F, D'Andrea M, et al. Predictive role of the UGT1A1, UGT1A7, and UGT1A9 genetic variants and their haplotypes on the outcome of metastatic colorectal cancer patients treated with fluorouracil, leucovorin, and irinotecan. *J Clin Oncol*. 2009;27:2457-2465.
48. van Schaik RH, van Agteren M, de Fijter JW, et al. UGT1A9 -275T>a/-2152C>T polymorphisms correlate with low MPA exposure and acute rejection in MMF/tacrolimus-treated kidney transplant patients. *Clin Pharmacol Ther*. 2009;86:319-327.
49. Sánchez-Frutoso AI, Maestro ML, Calvo N, et al. The prevalence of uridine diphosphate-glucuronosyltransferase 1A9 (UGT1A9) gene promoter region single-nucleotide polymorphisms T-275A and C-2152T and its influence on mycophenolic acid pharmacokinetics in stable renal transplant patients. *Transplant Proc*. 2009;41:2313-2316.
50. Kuypers DR, Naesens M, Vermeire S, Vanrenterghem Y. The impact of uridine diphosphate-glucuronosyltransferase 1A9 (UGT1A9) gene promoter region single-nucleotide polymorphisms T-275A and C-2152T on early mycophenolic acid dose-interval exposure in de novo renal allograft recipients. *Clin Pharmacol Ther*. 2005;78:351-361.
51. Sandanaraj E, Jada SR, Shu X, et al. Influence of UGT1A9 intronic I399C>T polymorphism on SN-38 glucuronidation in Asian cancer patients. *Pharmacogenomics J*. 2008;8:174-185.
52. Lu Y, Fang Y, Wu X, Ma C, Wang Y, Xu L. Effects of UGT1A9 genetic polymorphisms on monohydroxylated derivative of oxcarbazepine concentrations and oxcarbazepine monotherapy efficacy in Chinese patients with epilepsy. *Eur J Clin Pharmacol*. 2017;73:307-315.
53. Frechen S. UGT DDI inhibition qualification. 2020 Accessed July 4, 2022. <https://github.com/Open-Systems-Pharmacology/Qualification-DDI-UGT/releases/tag/v1.0>
54. Kanacher T, Lindauer A, Mezzalana E, et al. A physiologically-based pharmacokinetic (PBPK) model network for the prediction of CYP1A2 and CYP2C19 drug-drug-gene interactions with fluvoxamine, omeprazole, S-mephenytoin, Moclobemide, Tizanidine, Mexiletine, Ethinylestradiol, and caffeine. *Pharmaceutics*. 2020;12:12.
55. University of Washington. DDI—The Drug Interaction Database. 2022 Accessed December 8, 2022. <https://www.druginteractionsolutions.org/>
56. Centre UM. WHODrug Insight. Accessed July 4, 2022. <https://insight.who-umc.org/>
57. Trujillo ME, Arrington L, Patel Y, et al. Population pharmacokinetics of vericiguat in patients with heart failure with reduced ejection fraction: an integrated analysis. *Clin Pharmacol Ther*. 2022;112:1061-1069.

## SUPPORTING INFORMATION

Additional supporting information can be found online in the Supporting Information section at the end of this article.

**How to cite this article:** Frechen S, Ince I, Dallmann A, et al. Applied physiologically-based pharmacokinetic modeling to assess uridine diphosphate-glucuronosyltransferase-mediated drug–drug interactions for Vericiguat. *CPT Pharmacometrics Syst Pharmacol*. 2024;13:79-92. doi:[10.1002/psp4.13059](https://doi.org/10.1002/psp4.13059)